Polymer Testing 61 (2017) 373–377

Contents lists available at ScienceDirect

Polymer Testing

journal homepage: www.elsevier.com/locate/polytest

Test Method

Fatigue fracture of a highly stretchable acrylic elastomer

Wei Fan, Yang Wang, Shengqiang Cai*

Department of Mechanical and Aerospace Engineering, University of California, San Diego, La Jolla, CA 92093, USA

ARTICLE INFO

Article history:
Received 27 April 2017
Accepted 4 June 2017
Available online 8 June 2017

Keywords:
Dielectric elastomer
Fatigue fracture
Crack growth

ABSTRACT

Dielectric elastomer has been extensively explored in various applications as soft active material. In most applications, dielectric elastomer is subjected to cyclic loading-unloading condition. As a result, a small initial defect in a dielectric elastomer may finally grow to a critical size to induce catastrophic rupture. In this article, we carried out an experimental study of the crack growth in an acrylic dielectric elastomer under cyclic loading-unloading. Pure-shear test specimens were used to measure the relationship between crack growth rate and energy release rate. Such relationship can be simply fit to a power-law. We further used the measured power-law to successfully predict the fatigue lifetime of the acrylic elastomer with an edge crack and subject to simple extension cyclic loading-unloading test.

1. Introduction

Dielectric elastomer, as an electroactive polymer, has been recently explored in a variety of engineering applications ranging from soft actuators [1–13] to energy harvesting devices [14–20]. In most of the applications, dielectric elastomer films are subjected to cyclic loading-unloading. Consequently, a small initial defect in a dielectric elastomer may finally grow to a critical size to induce catastrophic rupture.

VHB 4910 (3M), an acrylic elastomer film, is a representative dielectric elastomer material under extensive investigations [1,13,21–23] Recently, rupture of VHB through one-time loading has been carefully studied in the experiments [24,25]. In particular, fracture energy of VHB was measured in the experiment, which has been shown to be independent of sample geometry [24]. In addition, stress softening phenomenon of VHB under cyclic loading-unloading has also been reported [26]. The stress for stretching a VHB film to a fixed strain decreases with the increase of cycle numbers and stabilizes after six loading-unloading cycles. However, according to our knowledge, no study has been conducted to characterize the kinetics of crack growth in a VHB film under cyclic loading-unloading condition.

In this article, pure-shear test specimens were employed to characterize the kinetics of crack growth in a VHB film under cyclic loading-unloading. Following the approach first proposed by Thomas [27], we measured the crack growth rate in a VHB film as a function of maximum energy release rate during the cyclic loading-unloading test. We then used the measured relationship between crack growth rate and maximum energy release rate to successfully predict the fatigue lifetime of the VHB film with an edge crack and subject to simple extension cyclic loading-unloading tests.

2. Experiments

2.1. Material and geometry

In the experiments, acrylic elastomer film VHB 4910 was purchased from 3M Company. We coated a thin layer of chalk powders on the surface of VHB sheets to enhance their visual contrast from the background. The VHB films were cut into different shapes for pure-shear test and simple extension test. Samples of both geometries were cyclically loaded-unloaded with and without a pre-cut. We denote the length, height and thickness of all samples in the undeformed state by L, H and T, and the initial crack length in a pre-cut sample by c_0. For pure-shear test, $T = 1$ mm, $L = 50$ mm and $H = 5$ mm. The schematics of the pristine sample and the sample with a pre-cut $c_0 = 20$ mm were shown in Fig. 1(a) and (b). For simple extension test, long-strip VHB samples were prepared with $T = 1$ mm, $L = 10$ mm and $H = 20$ mm, and an edge crack with $c_0 = 1$ mm was introduced to a pre-cut sample. Before the test, a VHB film was glued onto acrylic plates which were further clamped by the grippers of the mechanical testing machine (Instron 5965) with a 1 kN load cell.

* Corresponding author. Room 283, Engineering Building-II, 9500 Gilman Dr. #0411, La Jolla, CA 92093-0411, USA.
E-mail address: shqcai@ucsd.edu (S. Cai).

http://dx.doi.org/10.1016/j.polymertesting.2017.06.005
0142-9418/

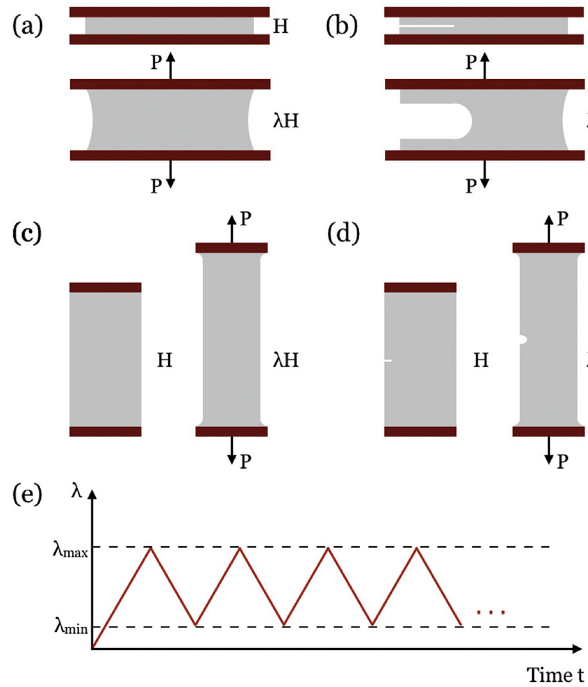

Fig. 1. Schematics of a VHB film subject to cyclic loading-unloading test. (a) A pristine VHB film under pure-shear test in undeformed state and deformed state; (b) A pre-cut VHB film under pure-shear test in undeformed state and deformed state; (c) Cyclic loading-unloading test with stretch rate: 1.8/s.

2.2. VHB thin films under cyclic loading-unloading tests

In pure-shear tests of VHB films with and without a pre-cut, stretch was varied between minimum stretch λ_{min} and maximum stretch λ_{max} cyclically with a constant stretch rate 1.8/s as shown in Fig. 1(c). For all pure-shear tests, λ_{min} was fixed to be 1.2, while λ_{max} is varied from 1.5 to 4.5. In simple extension tests, the cyclic loading-unloading process is similar to the pure-shear test with a constant stretch rate 1.8/s. For all simple extension tests, λ_{min} was fixed to be 1.2, while λ_{max} is varied from 2 to 4. During the tests, both stretch and force were recorded automatically by the Instron machine.

2.3. Crack growth in the specimen under cyclic loading-unloading test

A computer-controlled-camera system was used to record the crack growth process in the pure-shear specimen with a pre-cut. A Canon 60D digital camera was fixed at the same height as the testing sample, and faced to the front surface of the sample perpendicularly. Camera was activated periodically by a customized Matlab program to take photos. The period between each activation varied from 10 s to 150 s, depending on the specific cyclic test. During each activated state, the camera was set to take 10 photos continuously at high speed. All the photos were subsequently transferred to Black & White form, as shown in Fig. 2(a). Each photo contained the following information: the time t, stretch of the sample λ and crack length c. The information was extracted from the digital photos using the customized Matlab program. By converting time t to cycle N, we obtained crack length $c(\lambda, N)$ at stretch λ and cycle number N. The increase of crack length Δc is defined as $\Delta c(\lambda, N) = c(\lambda, N)\text{-}c_0$, which can be induced by both crack propagation and stretch of the sample. To capture the crack propagation, we further selected the data of Δc for a small and fixed stretch as $\lambda = 1.4$, as shown in Fig. 2(b). For a fixed λ_{max}, with a good approximation, the Δc increased linearly with the increase of number of cycles N. For different λ_{max}, Fig. 2(c) sketched the linear growth of Δc with the number of cycles N at fixed stretch 1.4. Consequently, the crack growth rate defined as dc/dN can be obtained by a linear fitting, $\Delta c(\lambda = 1.4, N)/N$.

3. Results and discussion

3.1. Energy release rate as a loading parameter for cyclic test

To characterize crack growth rate in a material subjected to cyclic loading-unloading, maximum energy release rate during a

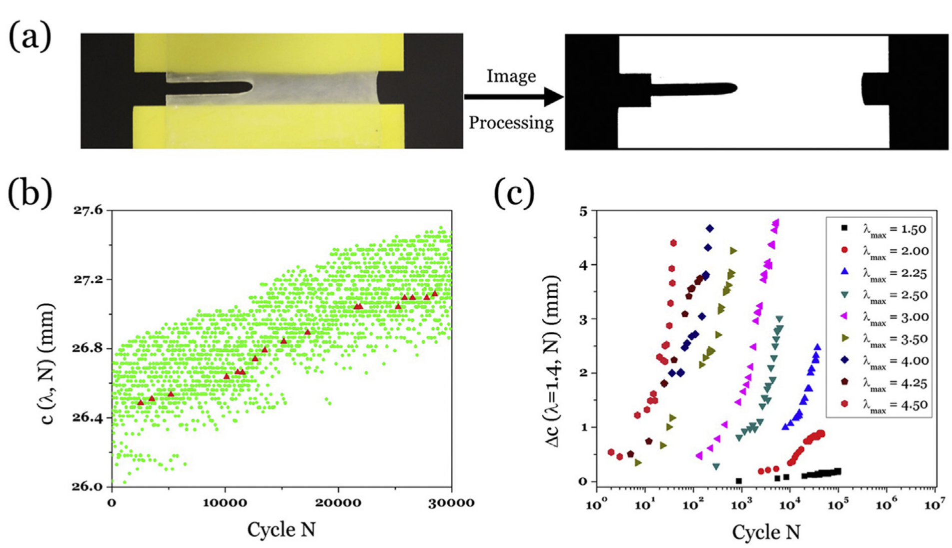

Fig. 2. Crack growth in a pre-cut VHB film subject to cyclic loading-unloading test. (a) For a pre-cut pure-shear VHB sample, photos are transferred to Black and White form to measure the crack length and calculate stretch; (b) A pre-cut pure-shear VHB sample subject to cyclic loading-unloading test with $\lambda_{min} = 1.2$ and $\lambda_{max} = 2$, and crack length c varies with stretch λ and cycle number N. Green dots represent the crack length change in all stretches with different cycle number N. Red triangles represent the crack length change around stretch $\lambda = 1.4$ with different cycle number N; (c) In different cyclic tests, crack length change Δc around stretch $\lambda = 1.4$ is selected and shown as a function of cycle number N. (For interpretation of the references to colour in this figure legend, the reader is referred to the web version of this article.)

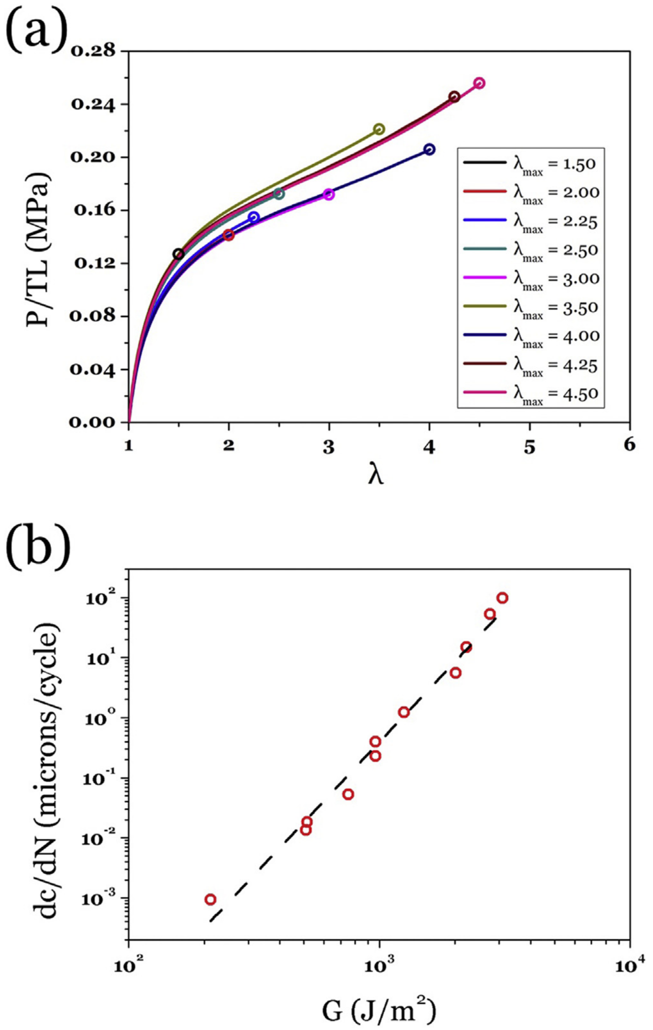

Fig. 3. (a) Stress-stretch curves of pristine VHB film subject to pure-shear test with different maximum stretches; (b) Dependence of crack growth rate on maximum energy release rate. Red cycles are experimental measurements. Black dash line is a fitting line. (For interpretation of the references to colour in this figure legend, the reader is referred to the web version of this article.)

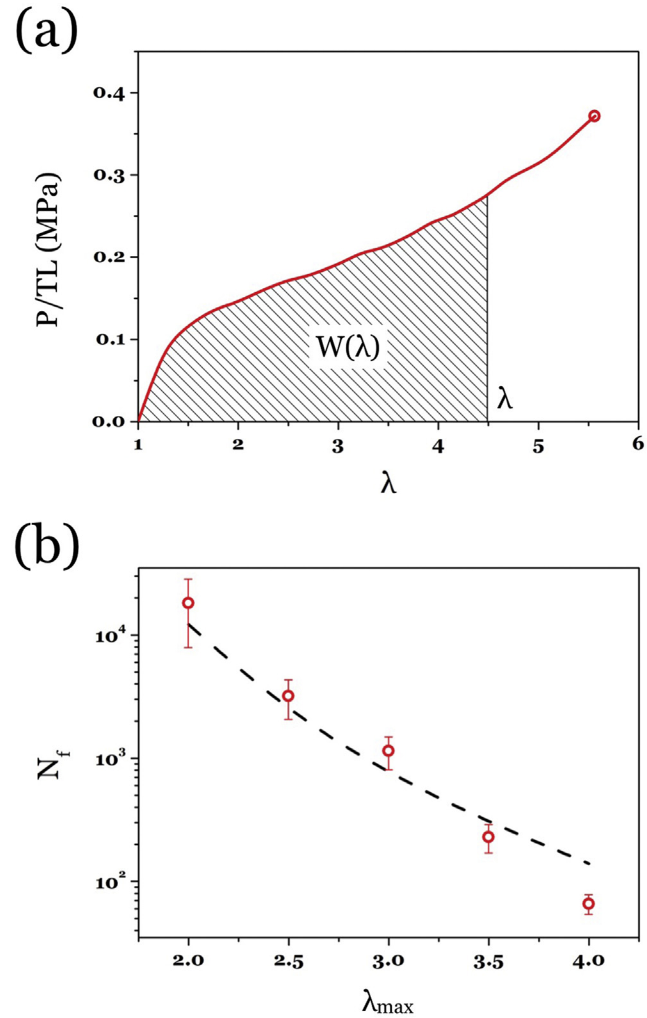

Fig. 4. (a) Measurement of strain energy for pristine VHB film under simple extension test; (b) Fatigue lifetime for VHB film with an edge crack with initial crack length $c_o = 1$ mm under cyclic loading-unloading simple extension test. The black dash line is prediction and red cycles are experimental measurements. (For interpretation of the references to colour in this figure legend, the reader is referred to the web version of this article.)

cyclic test has been commonly adopted as the loading parameter. It has been shown in various elastomers [27–30] the relationship between crack growth rate which is defined as the increase of crack length per cycle and maximum energy release rate can be usually fit to a power-law. It has also been shown in some studies that the ratio *R* between the minimum energy release rate and maximum energy release rate can affect the power-law [31,32].

In our experiments, we varied the maximum energy release rate *G* through controlling the maximum stretch λ_{max}. In the pure-shear test, maximum energy release rate can be computed by Ref. [33],

$$G(\lambda_{max}) = W(\lambda_{max}) \times H \tag{1}$$

where *H* is initial sample height and $W(\lambda_{max})$ is strain energy density measured from stress-stretch curve of pristine VHB 4910 sheet with the stretch λ_{max}. The stress-stretch curves of pristine VHB thin films with different maximum stretches are shown in Fig. 3(a). When the maximum stretch λ_{max} is varied from 1.5 to 4.5, the maximum energy release rate varied from 0.212 kJ/m^2 to 3.10 kJ/m^2 as calculated from Eq. (1). It is noted that the λ_{min} in the cyclic test was fixed as 1.2 in all the tests. Due to the plasticity of the elastomer, the VHB film is almost in a stress-free state when the stretch equals to λ_{min}. Therefore, the minimum energy release rate in all our tests was approximately zero.

3.2. Crack growth kinetics

Fig. 3(b) plots crack growth rate dc/dN as a function of maximum energy release rate $G(\lambda_{max})$. The measured relationship can be fit to a simple power law:

$$\frac{dc}{dN} = BG^F \tag{2}$$

where *B* and *F* are material parameters. For the VHB film tested in the current study, we obtain $B = 0.395$ (mm/kcycles) (kJ/m^2)$^{-F}$, $F = 4.43$. It is noted that in the fatigue tests of various rubbers [28,34], the value of *B* can vary significantly, while the value of *F* usually varies from 2 to 6. For example, $F = 2$ for nature rubber [28], which has also been used as dielectric elastomers [2,35].

3.3. Prediction of fatigue lifetime of VHB film during simple extension

With the above measurement of crack growth rate as a function of maximum energy release rate, we next try to predict the lifetime of an acrylic elastomer film subjected to simple extension cyclic loading-unloading tests. When a pre-existing crack in the film grows from the initial length c_0 to a critical length c_f, fast rupture happens and the material fails. The fatigue lifetime is defined as the total number of cycles N_f required for the crack length increasing from c_0 to c_f.

When an elastomer sheet with an edge crack subjected to simple extension, based on dimensional analysis, the energy release rate can be written as,

$$G = 2k(\lambda) \times W(\lambda) \times c \tag{3}$$

where c is the length of the crack, $k(\lambda)$ is a dimensionless function given by Lindley [36]: $k = (2.95 - 0.08 \times (\lambda - 1))/\lambda^{1/2}$ and $W(\lambda)$ is strain energy density measured from stress-stretch curve of a pristine sample under simple extension, as shown in Fig. 4(a). As crack length c increases to the critical size c_f, maximum energy release rate should be equal to fracture energy Γ of the elastomer. Therefore, the critical flaw size c_f can be calculated by,

$$c_f = \frac{\Gamma}{2k(\lambda_{max}) \times W(\lambda_{max})} \tag{4}$$

For VHB 4910, fracture energy Γ is given by Pharr [24] for about 5000 J/m^2 when stretch rate is 100/min.

A combination of Eqs. (2) and (3) gives that,

$$\frac{dc}{dN} = B \times (2k \times W \times c)^F \tag{5}$$

which can be used to predict the crack growth. Through integrating Eq. (5), we can obtain the fatigue lifetime of a VHB film with an edge crack and subject to simple extension as:

$$N_f = \int_0^{N_f} dN = \int_{c_o}^{c_f} \frac{1}{B(2kW)^F} c^{-F} dc = \frac{c_o^{1-F} - c_f^{1-F}}{B(F-1)(2kW)^F} \tag{6}$$

For simple extension tests of a VHB film with a pre-cut, the initial crack length $c_o = 1$ mm, and critical crack length c_f for different maximum stretch is calculated by Eq. (4). For each cyclic loading-unloading condition, three identical tests were repeated. The predicted fatigue lifetime from Eq. (6) as a function of maximum stretch λ_{max} was compared with experimental result, as shown in Fig. 4(b). It can be seen that the prediction fits well with the experiment, indicating that the measured power-law for crack growth in a VHB film as shown in Fig. 3(b) is indeed independent of sample geometry and specific stress state in the material.

4. Conclusion

In this article, we conducted experimental studies on the kinetics of crack growth in an acrylic elastomer (VHB 4910) subject to pure-shear cyclic loading-unloading test. We found that the relationship between crack growth rate and energy release rate can be simply described by a power-law. Using the measured power-law, we successfully predict the fatigue lifetime of the elastomer with an edge crack of different lengths and subject to simple extension cyclic loading-unloading test. The result can be important for the engineering applications of VHB, where cyclic loading-unloading is unavoidable.

Acknowledgement

S. Cai acknowledges the support from American Chemical Society through Award No. 55379-DNI9.

References

[1] R. Pelrine, R. Kornbluh, Q. Pei, J. Joseph, S. Park, T. Shrout, R.H. Baughman, Q.M. Zhang, V. Bharti, X. Zhao, M. Zhenyi, T. Furukawa, N. Seo, E. Smela, O. Inganäs, I. Lundström, E. Smela, N. Gadegaard, T. Otero, H.B. Schreyer, K. Oguro, H. Tamagawa, R. Kornbluh, R. Pelrine, R. Heydt, High-speed electrically actuated elastomers with strain greater than 100%, Science 287 (2000) 836–839, http://dx.doi.org/10.1126/science.287.5454.836.

[2] R. Pelrine, R. Kornbluh, J. Joseph, R. Heydt, Q. Pei, S. Chiba, High-field deformation of elastomeric dielectrics for actuators, Mat. Sci. Eng. C 11 (2000) 89–100, http://dx.doi.org/10.1016/S0928-4931(00)00128-4.

[3] R. Pelrine, R. Kornbluh, G. Kofod, High-strain actuator materials based on dielectric elastomers, Adv. Mater 12 (2000) 1223–1225, http://dx.doi.org/10.1002/1521-4095(200008)12:16<1223::AID-ADMA1223>3.0.CO;2–2.

[4] R. Pelrine, R.D.D. Kornbluh, Q. Pei, S. Stanford, S. Oh, J.J. Eckerle, R.J.J. Full, M.A. Rosenthal, K. Meijer, Dielectric elastomer artificial muscle actuators: toward biomimetic motion, Proc. SPIE 4695 (2002) 126–137, http://dx.doi.org/10.1117/12.475157.

[5] N. Galler, H. Ditlbacher, B. Steinberger, A. Hohenau, M. Dansachmüller, F. Camacho-Gonzales, S. Bauer, J.R. Krenn, A. Leitner, F.R. Aussenegg, Electrically actuated elastomers for electro-optical modulators, Appl. Phys. B Lasers Opt. 85 (2006) 7–10, http://dx.doi.org/10.1007/s00340-006-2434-4.

[6] S. Shian, R.M. Diebold, D.R. Clarke, Tunable lenses using transparent dielectric elastomer actuators, Opt. Express 21 (2013) 8669–8676, http://dx.doi.org/10.1364/OE.21.008669.

[7] F. Carpi, G. Frediani, S. Turco, R.D. De, Bioinspired tunable lens with muscle-like electroactive elastomers, Adv. Funct. Mat. 21 (2011) 4152–4158, http://dx.doi.org/10.1002/adfm.201101253.

[8] F. Carpi, R. Kornbluh, P. Sommer-Larsen, G. Alici, Electroactive polymer actuators as artificial muscles: are they ready for bioinspired applications? Bioinspir. Biomim. 6 (2011) 045006, http://dx.doi.org/10.1088/1748-3182/6/4/045006.

[9] S. Son, D. Pugal, T. Hwang, H.R. Choi, J.C. Koo, Y. Lee, K. Kim, J.-D. Nam, Electromechanically driven variable-focus lens based on transparent dielectric elastomer, Appl. Opt. 51 (2012) 2987–2996, http://dx.doi.org/10.1364/AO.51.002987.

[10] P. Brochu, Q. Pei, Advances in dielectric elastomers for actuators and artificial muscles, Macromol. Rapid Commun. 31 (2010) 10–36, http://dx.doi.org/10.1002/marc.200900425.

[11] I.A. Anderson, T.A. Gisby, T.G. McKay, B.M. O'Brien, E.P. Calius, Multi-functional dielectric elastomer artificial muscles for soft and smart machines, J. Appl. Phys. 112 (2012) 041101, http://dx.doi.org/10.1063/1.4740023.

[12] J. Rossiter, P. Walters, B. Stoimenov, Printing 3D dielectric elastomer actuators for soft robotics, Proc. SPIE 7287 (2009) 72870H, http://dx.doi.org/10.1117/12.815746.

[13] H.R. Choi, S.M. Ryew, K.M. Jung, H.M. Kim, J.W. Jeon, J.D. Nam, R. Maeda, K. Tanie, Soft actuator for robotic applications based on dielectric elastomer: quasi-static analysis, Proc. 2002 IEEE Int. Conf. Robot. Autom. 3 (2002) 3212–3217, http://dx.doi.org/10.1109/ROBOT.2002.1013721 (Cat. No.02CH37292).

[14] R. Peirine, R. Kornbluh, J. Eckerle, P. Jeuck, S. Oh, Q. Pei, S. Stanford, S.R.I. International, R. Avenue, M. Park, Dielectric elastomers: generator mode fundamentals and applications, Proc. SPIE 4329 (2001) 148–156, http://dx.doi.org/10.1117/12.432640.

[15] S. Chiba, M. Waki, R. Kornbluh, R. Pelrine, Innovative wave power generation system using electroactive polymer artificial muscles, Ocean (2009) 1–3, http://dx.doi.org/10.1109/OCEANSE.2009.5278346, 2009-EUROPE.

[16] S. Chiba, M. Waki, T. Wada, Y. Hirakawa, K. Masuda, T. Ikoma, Consistent ocean wave energy harvesting using electroactive polymer (dielectric elastomer) artificial muscle generators, Appl. Energy 104 (2013) 497–502, http://dx.doi.org/10.1016/j.apenergy.2012.10.052.

[17] R. Vertechy, M. Fontana, G.P.R. Papini, D. Forehand, In-tank tests of a dielectric elastomer generator for wave energy harvesting, Proc. SPIE 9056 (2014) 90561G, http://dx.doi.org/10.1117/12.2045046 doi:Artn 90561g\r.

[18] R. Vertechy, M. Fontana, G.P. Rosati Papini, M. Bergamasco, Oscillating-water-column wave-energy-converter based on dielectric elastomer generator, Proc. SPIE 8687 (2013) 86870I, http://dx.doi.org/10.1117/12.2012016.

[19] J. Maas, C. Graf, Dielectric elastomers for hydro power harvesting, Smart Mat. Struct. 21 (2012) 064006, http://dx.doi.org/10.1088/0964-1726/21/6/064006.

[20] C. Graf, J. Maas, D. Schapeler, Energy harvesting cycles based on electro active polymers, Proc. SPIE 7642 (2010) 1–12, http://dx.doi.org/10.1109/ICSD.2010.5568255.

[21] M. Wissler, E. Mazza, Electromechanical coupling in dielectric elastomer actuators, Sensors Actuators, A Phys. 138 (2007) 384–393, http://dx.doi.org/10.1016/j.sna.2007.05.029.

[22] M. Wissler, E. Mazza, Mechanical behavior of an acrylic elastomer used in dielectric elastomer actuators, Sensors Actuators, A Phys. 134 (2007) 494–504, http://dx.doi.org/10.1016/j.sna.2006.05.024.

[23] R. Shankar, T.K. Ghosh, R.J. Spontak, Mechanical and actuation behavior of electroactive nanostructured polymers, Sensors Actuators, A Phys. 151 (2009) 46–52, http://dx.doi.org/10.1016/j.sna.2009.01.002.
[24] M. Pharr, J.Y. Sun, Z. Suo, Rupture of a highly stretchable acrylic dielectric elastomer, J. Appl. Phys. 111 (2012) 104114, http://dx.doi.org/10.1063/1.4721777.
[25] A. Schmidt, P. Rothemund, E. Mazza, Multiaxial deformation and failure of acrylic elastomer membranes, Sensors Actuators, A Phys. 174 (2012) 133–138, http://dx.doi.org/10.1016/j.sna.2011.12.004.
[26] R.K. Sahu, K. Patra, Rate-dependent mechanical behavior of VHB 4910 elastomer, Mech. Adv. Mat. Struct. 23 (2016) 170–179, http://dx.doi.org/10.1080/15376494.2014.949923.
[27] A.G. Thomas, Cut growth in natural rubber vulcanizates, J. Polym. Sci. 31 (1958) 467–480, http://dx.doi.org/10.1002/pol.1958.1203112324.
[28] G.J. Lake, P.B. Lindley, The mechanical fatigue limit for rubber, J. Appl. Polym. Sci. 9 (1965) 1233–1251, http://dx.doi.org/10.1002/app.1965.070090405.
[29] A.N. Gent, P.B. Lindley, A.G. Thomas, Cut growth and fatigue of rubbers. I. The relationship between cut growth and fatigue, J. Appl. Polym. Sci. 8 (1964) 455–466, http://dx.doi.org/10.1002/app.1964.070080129.
[30] G.J. Lake, P.B. Lindley, Cut growth and fatigue of rubbers. II. Experiments on a noncrystallizing rubber, J. Appl. Polym. Sci. 8 (1964) 707–721, http://dx.doi.org/10.1002/app.1964.070080212.
[31] J.H. Fielding, Flex life and crystallization of synthetic rubber, Ind. Eng. Chem. 35 (1943) 1259–1261, http://dx.doi.org/10.1021/ie50408a008.
[32] P.B. Lindley, Non-relaxing crack growth and fatigue in a non-crystallizing rubber, Rubber Chem. Technol. 47 (1974) 1253–1264, http://dx.doi.org/10.5254/1.3540497.
[33] R.S. Rivlin, A.G. Thomas, Rupture of rubber. I. Characteristic energy for tearing, J. Polym. Sci. 10 (1953) 291–318, http://dx.doi.org/10.1002/pol.1953.120100303.
[34] G. Young, Dynamic property and fatigue crack propagation research on tire sidewall and model compounds, Rubber Chem. Technol. 58 (1985) 705–805.
[35] R. Kaltseis, C. Keplinger, S.J. Adrian Koh, R. Baumgartner, Y.F. Goh, W.H. Ng, A. Kogler, A. Tröls, C.C. Foo, Z. Suo, S. Bauer, Natural rubber for sustainable high-power electrical energy generation, RSC Adv. 4 (2014) 27905–27913, http://dx.doi.org/10.1039/C4RA03090G.
[36] P.B. Lindley, Energy for crack growth in model rubber components, J. Strain Anal. Eng. Des. 7 (1972) 132–140, http://dx.doi.org/10.1243/03093247V072132.